SUPPLEMENTARY INFORMATION

HEPATITIS B VIRUS-INDUCED ALTERATIONS IN HEPATOCYTE CD1D LIPID ANTIGENS ACTIVATE NATURAL KILLER T CELLS AND CONTRIBUTE TO PROTECTIVE IMMUNITY

Sebastian Zeissig[1,2], Kazumoto Murata[3], Lindsay Sweet[4], Jean Publicover[5], Zongyi Hu[3], Arthur Kaser[1], Esther Bosse[2], Jahangir Iqbal[6], M. Mahmood Hussain[6], Katharina Balschun[7], Christoph Röcken[7], Alexander Arlt[2], Rainer Günther[2], Jochen Hampe[2], Stefan Schreiber[2], Jody L. Baron[5], D. Branch Moody[4], T. Jake Liang[3,8], Richard S. Blumberg[1,8]

[1]Division of Gastroenterology, Hepatology, and Endoscopy, Brigham and Women's Hospital, Harvard Medical School, Boston, MA, USA.

[2]Department of Internal Medicine I, University Medical Center Schleswig-Holstein, Christian-Albrechts-University, Kiel, Germany.

[3]Liver Diseases Branch, NIDDK, National Institutes of Health, Bethesda, MD, USA.

[4]Division of Rheumatology, Immunology and Allergy, Brigham and Women's Hospital and Harvard Medical School, Boston, MA USA.

[5]Department of Medicine, Liver Center, University of California, San Francisco, CA, USA.

[6]Departments of Cell Biology and Pediatrics, SUNY Downstate Medical Center, Brooklyn, NY, USA.

[7]Department of Pathology, University Medical Center Schleswig-Holstein, Campus Kiel, Christian-Albrechts-University, Kiel, Germany.

[8]These authors share senior authorship.

1. Supplementary Data

Generation and description of 4Get mouse strains

Recently, Locksley et al. generated bicistronic mice expressing GFP via an internal ribosome entry site (IRES) in the IL-4 transcript (IL-4/GFP-enhanced transcript (4Get) mice) and demonstrated that these mice allow for detection of iNKT cells due to constitutive transcription of IL-4.[1,2] Analysis of 4Get liver mononuclear cells revealed that a fraction of GFP^+ cells did not react with αGalCer/CD1d tetramers (Suppl. Fig. 3a), thus representing either conventional $IL\text{-}4^+$ $CD4^+$ T cells or non-invariant NKT cells which, similar to iNKT cells, constitutively transcribe IL-4. To delineate these possibilities, we crossed 4Get mice with $J\alpha18^{-/-}$ mice that lack invariant but not non-invariant NKT cells due to knockout of the Jα segment of the semi-invariant T cell receptor. 4Get X $CD1d^{-/-}$ mice that lack both invariant and non-invariant NKT cells served as negative control. Analysis of 4Get X $J\alpha18^{-/-}$ mice revealed a significant population of GFP^+CD3^+ cells in thymus, spleen, liver and mesenteric lymph nodes that could not be detected in 4Get X $CD1d^{-/-}$ mice consistent with the presence of noninvariant NKT cells (Suppl. Fig. 3a-b). GFP^+CD3^+ cells expressed activation (CD69, CD25, CD44) and memory (CD45RO) markers consistent with an effector/memory phenotype, a hallmark of NKT cells (Figure 1d-f, Suppl. Fig. 4 and data not shown). In addition, 46±7 % of liver and 37±2 % of spleen GFP^+CD3^+ cells expressed the natural killer marker NK1.1. We tested CD1d-restriction of GFP^+CD3^+ cells obtained by flow cytometric sorting (purity 92-95%) of spleens from 4Get X $J\alpha18^{-/-}$ mice. We found that GFP^+CD3^+ but not GFP^-CD3^+ cells secreted IFN-γ in response to CD1d-transfected RMASd cells but not CD1d-deficient RMAS cells (Suppl. Fig. 3c). In addition, GFP^+ but not GFP^- cells responded to splenocytes in a CD1d-restricted manner as demonstrated by blocking with monoclonal antibodies directed against CD1d (Suppl. Fig. 3d). In contrast, rare splenic GFP^+CD3^+ cells obtained from 4Get X $CD1d^{-/-}$ mice did not exhibit CD1d-restricted activation (Suppl. Fig. 3c-d). These results demonstrate that 4Get X $J\alpha18^{-/-}$ mice allow for specific detection of noninvariant NKT cells. It should be noted, however, that other

subgroups of non-invariant NKT cells may exist which escape detection in this model due to lack of constitutive IL-4 transcription.

2. Supplementary Methods

Primary cells and cell lines

Primary human hepatocytes were obtained from Invitrogen (Carlsbad, CA). Primary murine hepatocytes were extracted as described before.[3] In addition, mock-transfected and CD1d-transfected RMA-S and RMA-Sd cells were used as antigen presenting cells.[4] Murine NKT cell hybridomas and human NKT cell lines were described before.[5-7] In addition, iNKT cells were obtained by α-galactosylceramide-driven expansion of Vα24-positive peripheral blood mononuclear cells obtained from healthy controls as previously described.[8,9] RF33.70 was used as a T cell hybridoma that recognizes the SIINFEKL peptide in the context of H-2Kb.[10]

Lipids and chemical inhibitors

All lipids were obtained from Avanti Polar Lipids unless mentioned otherwise. α-galactosylceramide was obtained from Kirin Brewery, Co. Ltd. (Tokyo, Japan). MTP was purified from bovine livers (M.M.H.) and was used at 500 ng/well (96 well plates) as described before.[11] MTP inhibitors BMS212122[12], BMS197636[13], BMS200150[13,14], the structurally related negative compound 9-fluorenyl carboxylic acid and their application for inhibition of CD1d-restricted antigen presentation[9,11,15,16] have been described. AACOCF3, AACOCH3, and MAFP were obtained from Enzo Life Sciences (Lörrach, Germany). sPLAII inhibitor c(2NapA)LS(2NapA)R was obtained from Merck Chemicals (Darmstadt, Germany).

Viral constructs, infection

The parental plasmid for HBV constructs was pGEM7-HBV1.3 containing a 1.3-fold-overlength genome of HBV, subtype *ayw*, with a 5′ terminal redundancy encompassing enhancers I and II, the

origin of replication (direct repeats DR1 and DR2), the X- and pregenomic/core promoter regions, the transcription initiation site of the pregenomic RNA, the unique polyadenylation site, and the entire X open reading frame. To generate HBV mutants, point mutations were introduced using the QuickChange II site-directed mutagenesis kit and protocol (Agilent Technologies, Santa Clara, CA) at the 19th codon of preS1 gene from TTG to TAG (L-) or at the initiation codon of pre-S2 and S from ATG to GTG (M- and S-). The PreS1 myristylation-defective (myr-) mutation was generated by changing the second codon of the preS1 gene from GGG (glycine) to GCG (alanine).

For generation of recombinant adenovirus genomes, the AdEasy system was employed (Agilent Technologies).[17] Briefly, the original and mutant 1.3-fold-overlength HBV mutant genomes were subcloned into the multiple-cloning site of the shuttle plasmid pAdTrack. Adenoviruses were obtained by homologous recombination of the shuttle plasmids and the adenoviral backbone plasmid pAdEasy1. Linearized recombinant adenovirus genomes were transfected into 293 cells for the generation and propagation of the recombinant adenoviruses. The resulting viruses were further amplified in 293 cells, purified with the AdEasy purification kit (Agilent Technologies) and titered by GFP. The resulting viruses are Ad-HBV L-M+S+, Ad-HBV L+M-S+, Ad-HBV L+M+S-, Ad-HBV myr-. The control virus expressing ß-galactosidase is Ad-LacZ. Ad-HBV and AdHBV L-M-S+ were obtained from Ulrike Protzer (TU München) and were prepared as described above.[18]

For *in vivo* experiments, mice were infected by tail vein injection of 1×10^9 Ad-HBV or Ad-LacZ viruses unless mentioned otherwise. In some experiments, neutralization of IL-12 was performed by i.v. injection of 300 μg of monoclonal anti-IL-12 p40 antibody (clone C17.8, eBioscience) two hours before i.v. injection of adenoviruses, lipopolysaccharide (Sigma-Aldrich, 40 μg/mouse), and α-galactosylceramide (2.5 μg/mouse). For *in vitro* infection, hepatocytes were exposed to a multiplicity of infection (MOI) of 20 for 12 hours before washing. Similarly, an MOI of 20 was used for infection of primary human hepatocytes with Ad-HBV, Ad-LacZ, and a primary HBV isolate (genotype A).

Determination of ALT, HBsAg, HBV DNA levels and liver histology

At the indicated days after *in vivo* infection with Ad-HBV and the respective controls, alanine aminotransferase (ALT/SGPT Liqui-UV Test, Stanbio, Boerne, TX) and HBsAg levels (GS HBsAg EIA 3.0, Biorad, Hercules, CA) were determined by ELISA according to the manufacturer's instructions. For determination of HBV DNA levels, DNA was extracted from serum and liver tissue using the QIAGEN QIAamp DNA Mini Kit (Qiagen Inc., Hilden, Germany) and HBV DNA was quantified by qPCR as described by Thimme et al.[19] Liver histology was scored in a blinded fashion by pathologists (K.B., C.R.) using the modified HAI score described by Ishak et al.[20] Immunohistochemical staining of HBcAg was done according to the manufacturer's instruction using a rabbit anti-HBcAg antibody (Dako Deutschland GmbH, Hamburg).

Flow cytometry

Cells were incubated with FcR blocking reagent (Miltenyi Biotec, Auburn, CA) and, for tetramer stainings, with 1 µg/ml unlabeled streptavidin (Pierce Biotechnology, Inc., Rockford, IL) for 15 min at 4°C before staining with monoclonal antibodies for 30 min at 4°C. Staining with CD1d-α-galactosylceramide (αGalCer) tetramers (1h, 4°C, NIH Tetramer Core Facility) was performed to detect invariant NKT (iNKT) cells. Cells were then washed and analyzed by flow cytometry using a four laser LSRII (BD Biosciences, San Jose, CA) and Flowjo software (Tree Star, Inc., Ashland, OR). For intracellular stainings, cells were first surface-stained, then permeabilized with Cytofix/Cytoperm (BD Biosciences) and washed with Perm/Wash buffer (BD Biosciences) according to the manufacturer's instructions. Antibodies were added for 30 min at 4°C before washing with Perm/Wash buffer. Intracellular cytokine stainings were performed without restimulation of cells and without inhibition of protein secretion. All antibodies and reagents used for flow cytometry were obtained from BD Biosciences except for CD1d-αGalCer tetramers (NIH Tetramer Core Facility). Via-Probe (BD Biosciences), and for intracellular stainings fixable viability dye eFluor 450 (eBiosciences), was added to all stainings for exclusion of dead cells.

Preparation and separation of cellular and microsomal lipids.

For extraction of microsomal lipids, primary hepatocytes were obtained as described above, microsomes were extracted according to Ernster et al.[21] and lipids were extracted following the Folch protocol.[22] Total hepatocyte lipids were extracted in a similar manner. Separation of lipids according to solubility was done as described in [23]. Briefly, microsomal lipids were dried, weighed, resuspend in chloroform and 2mg of microsomal lipids were applied to an open silica column (230-400 mesh, Sigma-Aldrich, St. Louis, MO). Lipids were eluted according to solubility by application of six fractions of each HPLC grade chloroform, acetone, and methanol (Sigma-Aldrich). Fractionated lipids were dried, weighed and loaded onto plate-bound CD1d.

Antigen presentation

Antigen presentation assays were performed in 96 well flat bottom plates using $2x10^4$ hepatocytes, $5x10^4$ RMA-S/d cells, $1x10^5$ splenocytes or hepatic mononuclear cells and, as responders, $1x10^5$ NKT cells or NKT cell hybridoma cells. Cytokine secretion was determined by ELISA after 16 hours of coculture (BD Biosciences). In some experiments, MTP inhibitors were added at a final concentration of 10 μM (BMS212122, BMS200150) and 100 nM (BMS197636), respectively. Alternatively, purified monoclonal CD1d blocking antibodies (1B1 clone, 19G11 clone) were used at a final concentration of 10 μg/ml.

For cell-free antigen presentation assays, monomeric mouse CD1d (NIH Tetramer Core Facility) was loaded onto 96 well flat bottom plates (0.25 μg/well), unbound CD1d was washed off, and lipids were added at a molar ratio of 40 :1. Unbound lipids were then washed off, NKT cells were added and cytokine secretion was determined by ELISA as described above. In some experiments, MTP purified from bovine liver (M.M.H.) was added at a final concentration of 500 ng/ml. In addition, in some experiments, GFP^+ αGalCer/CD1d-$tetramer^+$ 4Get invariant NKT cells and GFP^+ 4Get X $J\alpha18^{-/-}$ noninvariant NKT cells were sorted from liver mononuclear cells using a BD

Biosciences FACSAria II cell sorter and were used as responders in antigen presentation assays. Flow cytometric determination of cell surface CD69 and intracellular IFN-γ expression on GFP^+CD3^+ NKT cells was studied as readout. For *in vitro* neutralization of IL-12, a monoclonal anti-IL-12 p40 antibody (clone C17.8, eBioscience) was used at a final concentration of 10 μg/ml.

For ELISpot, liver and spleen mononuclear cells were isolated from mice at the indicated days after infection with adenoviruses and $2x10^5$ mononuclear cells were loaded onto IFN-γ ELISPOT plates (R&D Systems, Minneapolis, MN) together with the indicated HBV surface and core peptides[24] (1 μg/ml, JPT Peptide Technologies, Berlin, Germany). Plates were developed according to the manufacturer's instructions after 16 hours of stimulation. For ELISpot analysis using HBV envelope peptide pools please refer to [25].

Protein extraction, western blotting

Protein extraction and western blotting were performed as described previously.[26] The following antibodies were used: Rabbit anti-GFP, rabbit anti-calnexin, mouse anti-golgi 58K, mouse anti-beta actin, rabbit anti-LAMP-1 (all from Sigma-Aldrich), mouse anti-MTP (BD Biosciences), mouse anti-histone H1 (Santa Cruz Biotechnology Inc., Santa Cruz, CA).

Real-time PCR

Total RNA isolation and reverse transcription were performed using the RNeasy mini kit (Qiagen Inc., Hilden, Germany) and High-Capacity cDNA archive kit (Life Technologies Corporation, Carlsbad, CA) according to the manufacturers' instructions. Primer sequences were obtained from PrimerBank[27] and sequences are listed in Suppl. Table 1. Real-time PCR was performed using iQ SYBR Green Supermix (Biorad) and a Biorad MyiQ™2 system. β-actin served as endogenous control and was not altered in expression by the experimental conditions. PCR was set up in triplicates and threshold cycle (Ct) values of the target genes were normalized to the endogenous control. Differential expression was calculated according to the $2^{-\Delta\Delta CT}$ method.[28]

References

1. Mohrs, M., Shinkai, K., Mohrs, K. & Locksley, R.M. Analysis of type 2 immunity in vivo with a bicistronic IL-4 reporter. *Immunity* **15**, 303-311 (2001).
2. Stetson, D.B.*, et al.* Constitutive cytokine mRNAs mark natural killer (NK) and NK T cells poised for rapid effector function. *J Exp Med* **198**, 1069-1076 (2003).
3. Scapa, E.F.*, et al.* Regulation of energy substrate utilization and hepatic insulin sensitivity by phosphatidylcholine transfer protein/StarD2. *FASEB J* **22**, 2579-2590 (2008).
4. Teitell, M.*, et al.* Nonclassical behavior of the mouse CD1 class I-like molecule. *J Immunol* **158**, 2143-2149 (1997).
5. Behar, S.M., Podrebarac, T.A., Roy, C.J., Wang, C.R. & Brenner, M.B. Diverse TCRs recognize murine CD1. *J Immunol* **162**, 161-167 (1999).
6. Park, S.H., Roark, J.H. & Bendelac, A. Tissue-specific recognition of mouse CD1 molecules. *J Immunol* **160**, 3128-3134 (1998).
7. Brigl, M.*, et al.* Conserved and heterogeneous lipid antigen specificities of CD1d-restricted NKT cell receptors. *J Immunol* **176**, 3625-3634 (2006).
8. Exley, M.A., Balk, S.P. & Wilson, S.B. Isolation and Functional Use of Human NK T Cells. in *Current Protocols in Immunology* (Wiley, 2002).
9. Zeissig, S.*, et al.* Primary deficiency of microsomal triglyceride transfer protein in human abetalipoproteinemia is associated with loss of CD1 function. *J Clin Invest* **120**, 2889-2899 (2010).
10. Rock, K.L., Rothstein, L. & Gamble, S. Generation of class I MHC-restricted T-T hybridomas. *J Immunol* **145**, 804-811 (1990).
11. Dougan, S.K.*, et al.* Microsomal triglyceride transfer protein lipidation and control of CD1d on antigen-presenting cells. *J Exp Med* **202**, 529-539 (2005).
12. Robl, J.A.*, et al.* A novel series of highly potent benzimidazole-based microsomal triglyceride transfer protein inhibitors. *J Med Chem* **44**, 851-856 (2001).

13. Wetterau, J.R., *et al.* An MTP inhibitor that normalizes atherogenic lipoprotein levels in WHHL rabbits. *Science* **282**, 751-754 (1998).

14. Jamil, H., *et al.* An inhibitor of the microsomal triglyceride transfer protein inhibits apoB secretion from HepG2 cells. *Proc Natl Acad Sci U S A* **93**, 11991-11995 (1996).

15. Dougan, S.K., Rava, P., Hussain, M.M. & Blumberg, R.S. MTP regulated by an alternate promoter is essential for NKT cell development. *J Exp Med* **204**, 533-545 (2007).

16. Kaser, A., *et al.* Microsomal triglyceride transfer protein regulates endogenous and exogenous antigen presentation by group 1 CD1 molecules. *Eur J Immunol* **38**, 2351-2359 (2008).

17. He, T.C., *et al.* A simplified system for generating recombinant adenoviruses. *Proc Natl Acad Sci U S A* **95**, 2509-2514 (1998).

18. Sprinzl, M.F., Oberwinkler, H., Schaller, H. & Protzer, U. Transfer of hepatitis B virus genome by adenovirus vectors into cultured cells and mice: crossing the species barrier. *J Virol* **75**, 5108-5118 (2001).

19. Thimme, R., *et al.* CD8(+) T cells mediate viral clearance and disease pathogenesis during acute hepatitis B virus infection. *J Virol* **77**, 68-76 (2003).

20. Ishak, K., *et al.* Histological grading and staging of chronic hepatitis. *J Hepatol* **22**, 696-699 (1995).

21. Ernster, L., Siekevitz, P. & Palade, G.E. ENZYME-STRUCTURE RELATIONSHIPS IN THE ENDOPLASMIC RETICULUM OF RAT LIVER : A Morphological and Biochemical Study. *J Cell Biol* **15**, 541-562 (1962).

22. Folch, J., Lees, M. & Sloane Stanley, G.H. A simple method for the isolation and purification of total lipides from animal tissues. *J Biol Chem* **226**, 497-509 (1957).

23. Gumperz, J.E., *et al.* Murine CD1d-restricted T cell recognition of cellular lipids. *Immunity* **12**, 211-221 (2000).

24. von Freyend, M.J*., et al.* Sequential control of hepatitis B virus in a mouse model of acute, self-resolving hepatitis B. *J Viral Hepat* **18**, 216-226 (2011).

25. Publicover, J*., et al.* IL-21 is pivotal in determining age-dependent effectiveness of immune responses in a mouse model of human hepatitis B. *J Clin Invest* **121**, 1154-1162 (2011).

26. Zeissig, S*., et al.* Changes in expression and distribution of claudin 2, 5 and 8 lead to discontinuous tight junctions and barrier dysfunction in active Crohn's disease. *Gut* **56**, 61-72 (2007).

27. Spandidos, A., Wang, X., Wang, H. & Seed, B. PrimerBank: a resource of human and mouse PCR primer pairs for gene expression detection and quantification. *Nucleic Acids Res* **38**, D792-799 (2010).

28. Livak, K.J. & Schmittgen, T.D. Analysis of relative gene expression data using real-time quantitative PCR and the 2(-Delta Delta C(T)) Method. *Methods* **25**, 402-408 (2001).

3. Supplementary Figures

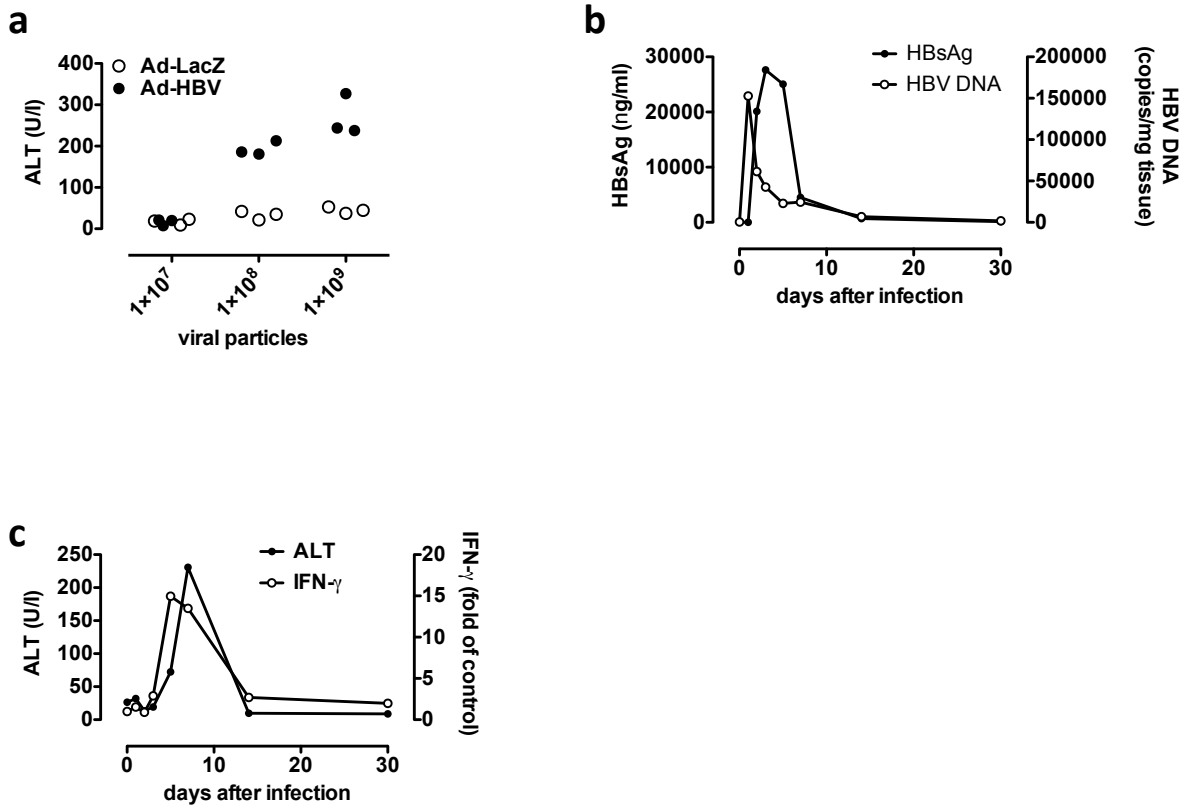

Suppl. Fig. 1. Ad-HBV but not Ad-LacZ induces hepatitis. (a) ALT release as determined seven days after i.v. administration of the indicated number of viral particles. (b-c) Serum HBsAg (b), liver HBV DNA (b), serum ALT (c), and liver IFN-γ (c) following Ad-HBV infection. Results are representative of two independent experiments.

Nature Medicine doi:10.1038/nm.2811

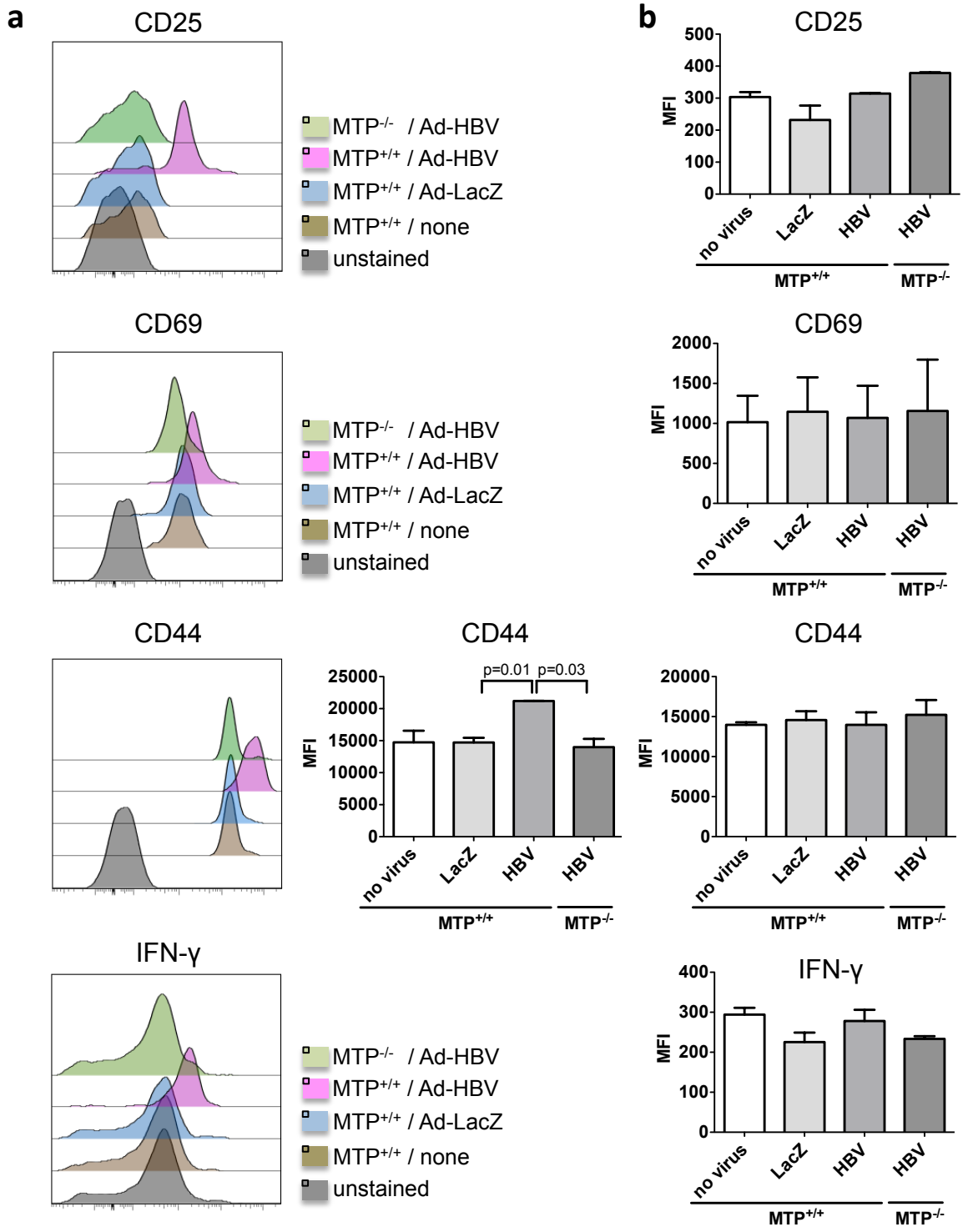

Suppl. Figure 2. HBV infection leads to activation and IFN-γ secretion of hepatic but not splenic iNKT cells. Hepatic (a) and splenic (b) iNKT cell (αGalCer/CD1d^{+}CD3^{+}) surface expression of activation markers CD25, CD69, CD44 and intracellular expression of interferon-γ (IFN-γ) two days after i.v. administration of PBS (no virus) or 1x10^{9} Ad-HBV or Ad-LacZ particles into H-*Mttp*$^{-/-}$ (MTP$^{-/-}$) and wildtype (MTP$^{+/+}$) mice. IFN-γ staining was performed without restimulation or brefeldin A treatment. Bar graphs of mean fluorescence intensities (MFI, mean ± s.e.m, 4-6 mice/group) and histogram plots of individual mice are shown. Data are from the same experiment as shown in Figure 1 and bar graphs of CD25, CD69, and IFN-γ expression of hepatic iNKT cells are shown in Fig. 1a-c. Results are representative of three independent experiments.

Nature Medicine doi:10.1038/nm.2811

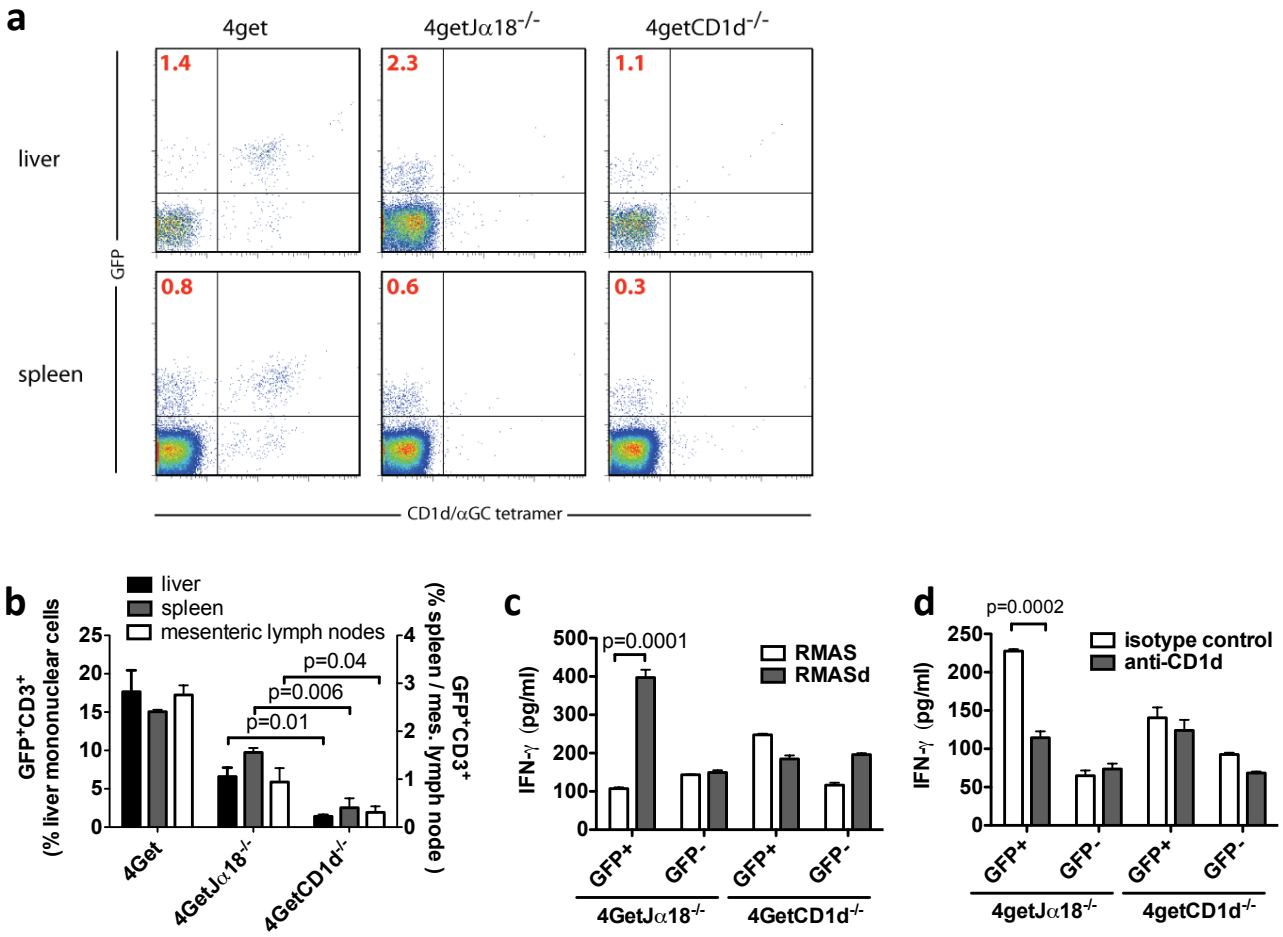

Suppl. Figure 3. Characterization of 4get models. (a) Dot plots of liver and spleen mononuclear cells from individual mice of the indicated mouse strains. Plots are gated on $CD3^+$ cells. Red numbers show the percentage of CD1d/αGalCer-negative GFP^+ cells. (b) Quantification of GFP^+CD3^+ cells among liver, spleen and mesenteric lymph node mononuclear cells of the indicated mouse strains (mean ± s.e.m, 5-6 mice/group). (c-d) GFP^+ and GFP^- $CD3^+$ splenocytes from the indicated strains were sorted by flow cytometry and cocultured for 24 h with untransfected (RMAS) and CD1d-transfected (RMASd) cells (c) or autologous irradiated splenocytes in the presence or absence of monoclonal antibodies directed against CD1d (d). IFN-γ secretion was determined by ELISA (mean ± s.e.m of triplicate cultures). Results are representative of two independent experiments.

Nature Medicine doi:10.1038/nm.2811

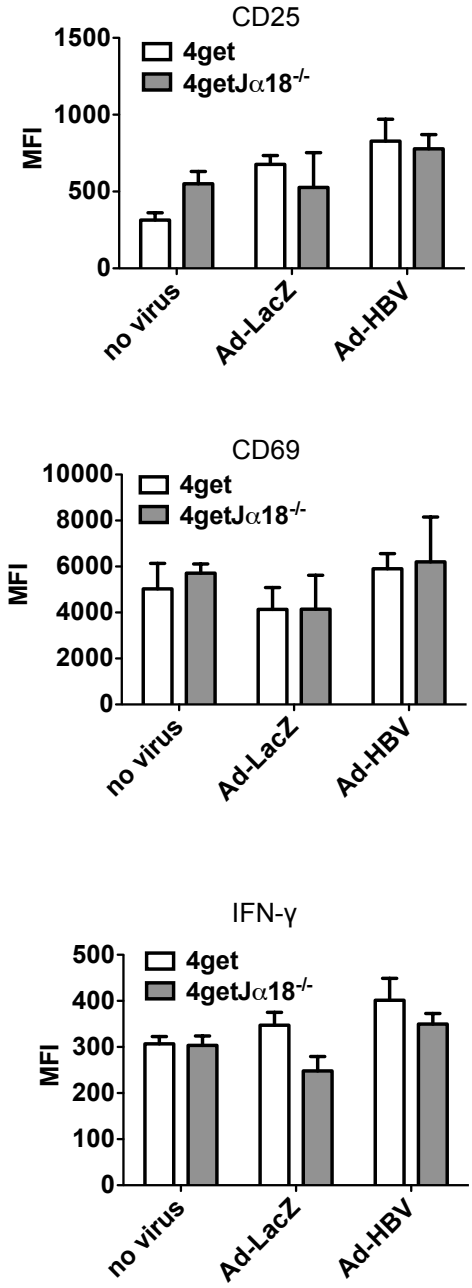

Suppl. Fig. 4. Lack of activation of splenic noninvariant NKT cells in response to Ad-HBV infection. Splenic non-invariant NKT cells (4getJα18$^{-/-}$) or total NKT cells (4get) two days after i.v. administration of PBS (no virus), Ad-HBV or Ad-LacZ. IFN-γ staining was performed without restimulation or brefeldin A treatment. Shown is the mean fluorescence intensity (MFI, mean ± s.e.m, 4-6 mice/group). Results are representative of three independent experiments.

Nature Medicine doi:10.1038/nm.2811

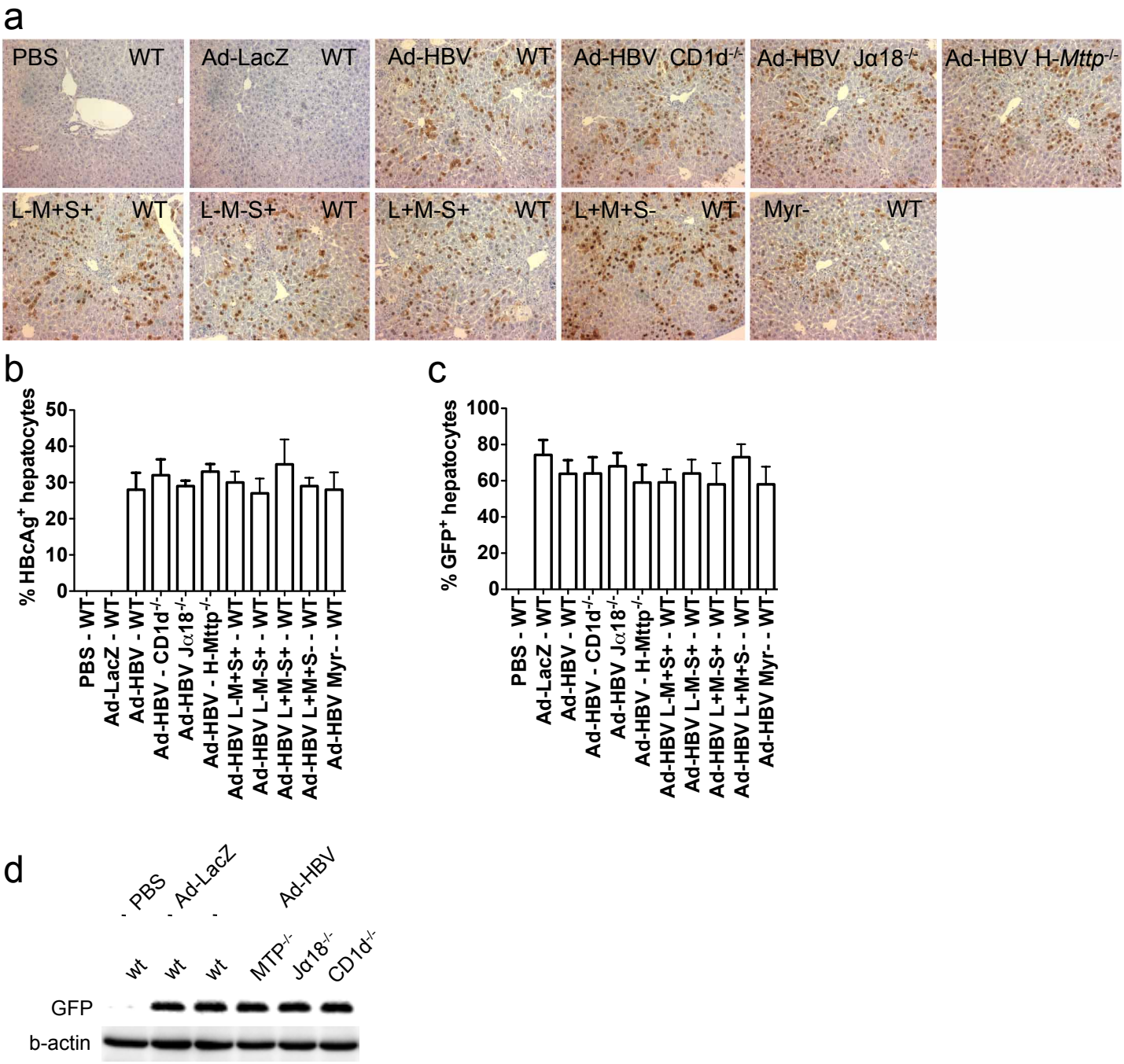

Suppl. Fig. 5. Expression of HBcAg and GFP in livers following transduction with Ad-LacZ, Ad-HBV and Ad-HBV mutants in wildtype, CD1d$^{-/-}$, Jα18$^{-/-}$, and H-*Mttp*$^{-/-}$ mice. Wildtype C57BL/6J mice or the respective knockout strains were injected i.v. with PBS or 1x10^{9} particles of the indicated adenoviruses. Two days after injection, livers were stained for HBcAg using fixed, paraffin-embedded tissue (a, b) or analyzed for native GFP expression in formalin-fixed cryosections (c). The mean percentage (± s.e.m.) of HBcAg- and GFP-positive hepatocytes is shown in (b) and (c), respectively. (d) Western blot of adenovirus-derived GFP in whole cell lysates of livers two days after *in vivo* transduction with Ad-LacZ and Ad-HBV. Results are representative of two independent experiments.

Nature Medicine doi:10.1038/nm.2811

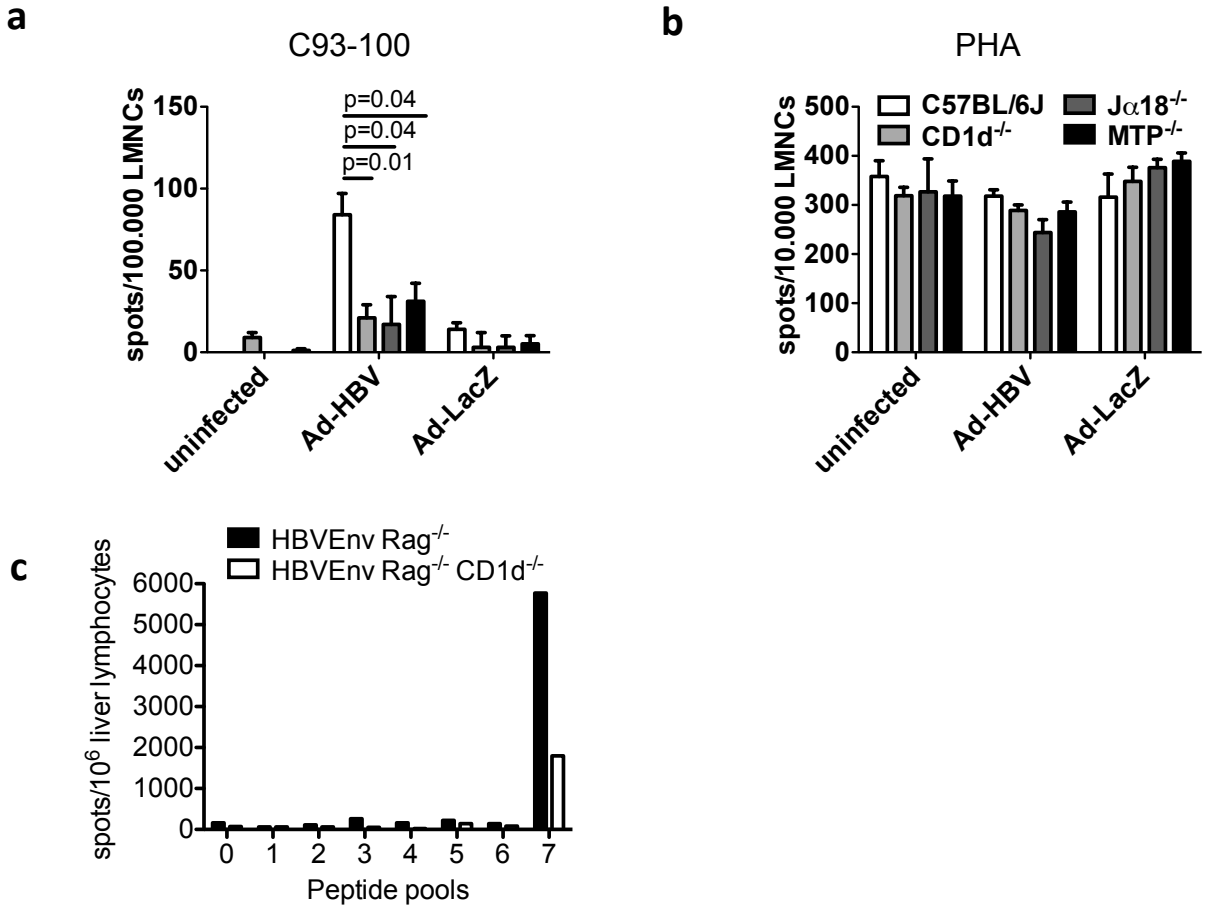

Suppl. Fig. 6. HBV-specific and non-specific immune responses. (a-b) IFN-γ secretion of LMNCs after *in vitr*o stimulation with the indicated HBV core-derived peptide (a) or PHA (b) 14 days after infection with Ad-HBV, Ad-LacZ or control. (c) Liver mononuclear cells obtained one year after wildtype splenocyte transfer into HBV envelope x Rag1$^{-/-}$ x CD1d$^{-/-}$ (HBVEnvRag$^{-/-}$) and HBV envelope x Rag1$^{-/-}$ (HBVEnvRag$^{-/-}$CD1d$^{-/-}$) mice on C57BL/6 background were restimulated in the presence of the indicated HBV envelope peptide pools and IFN-γ-secreting cells were detected by ELISpot. Results are representative of three independent experiments.

Nature Medicine doi:10.1038/nm.2811

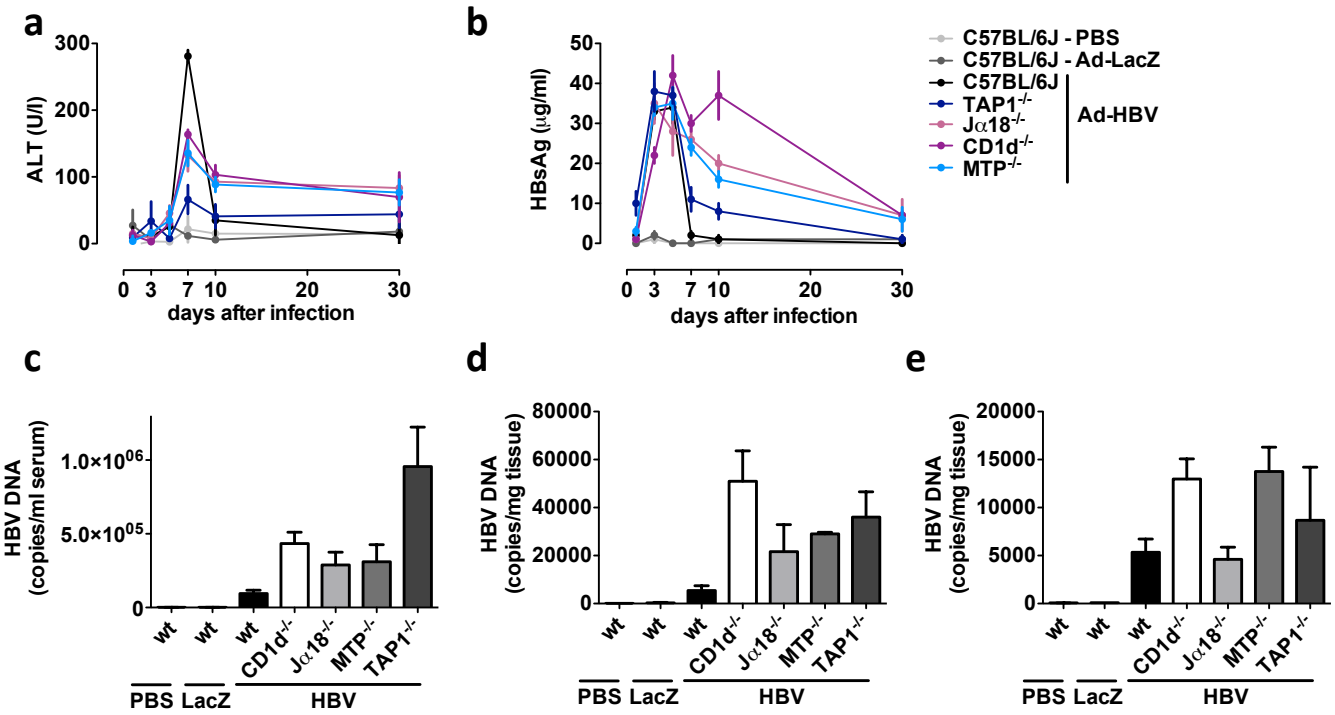

Suppl. Fig. 7. Alanine aminotransferase (a), serum HBsAg (b), serum HBV DNA (c), and liver HBV DNA on day 7 (d) and 14 (e) following i.v. administration of PBS, Ad-LacZ, and Ad-HBV. The same experiment as shown in Fig. 2 but including *Tap1*$^{-/-}$ mice. Mean ± s.e.m. is shown (6-8 mice per group). Results are representative of two independent experiments.

Nature Medicine doi:10.1038/nm.2811

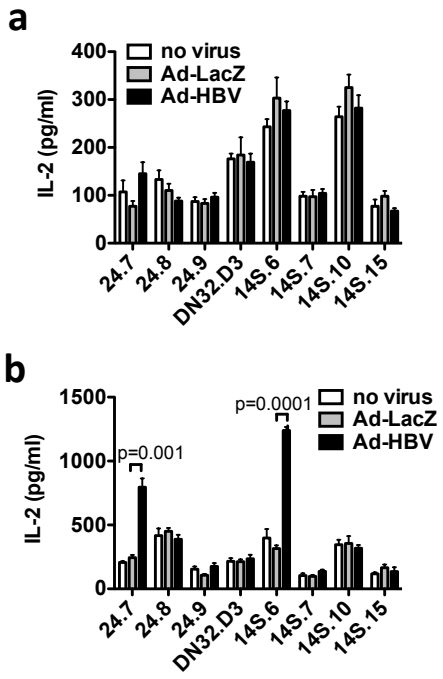

Suppl. Fig. 8. HBV infection leads to activation of invariant and non-invariant NKT cells by hepatocytes and not professional antigen presenting cells. (a) Unaltered CD1d-restricted antigen presentation by irradiated, T cell-depleted liver mononuclear cells of mice infected *in vivo* with Ad-HBV and Ad-LacZ as detected by IL-2 release (ELISA) of co-cultured invariant (24.7, 24.8, 24.9, DN32.D3) and non-invariant (14S.6, 14S.7, 14S.10, 14S.15) NKT hybridomas for 24h. (b) Selective activation of 24.7 and 14S.6 NKT hybridomas upon coculture with primary hepatocytes infected *in vitro* at a multiplicity of infection (MOI) of 20 with Ad-LacZ and Ad-HBV. Mean ± s.e.m. of triplicate cultures are shown. Three independent experiments were performed.

Nature Medicine doi:10.1038/nm.2811

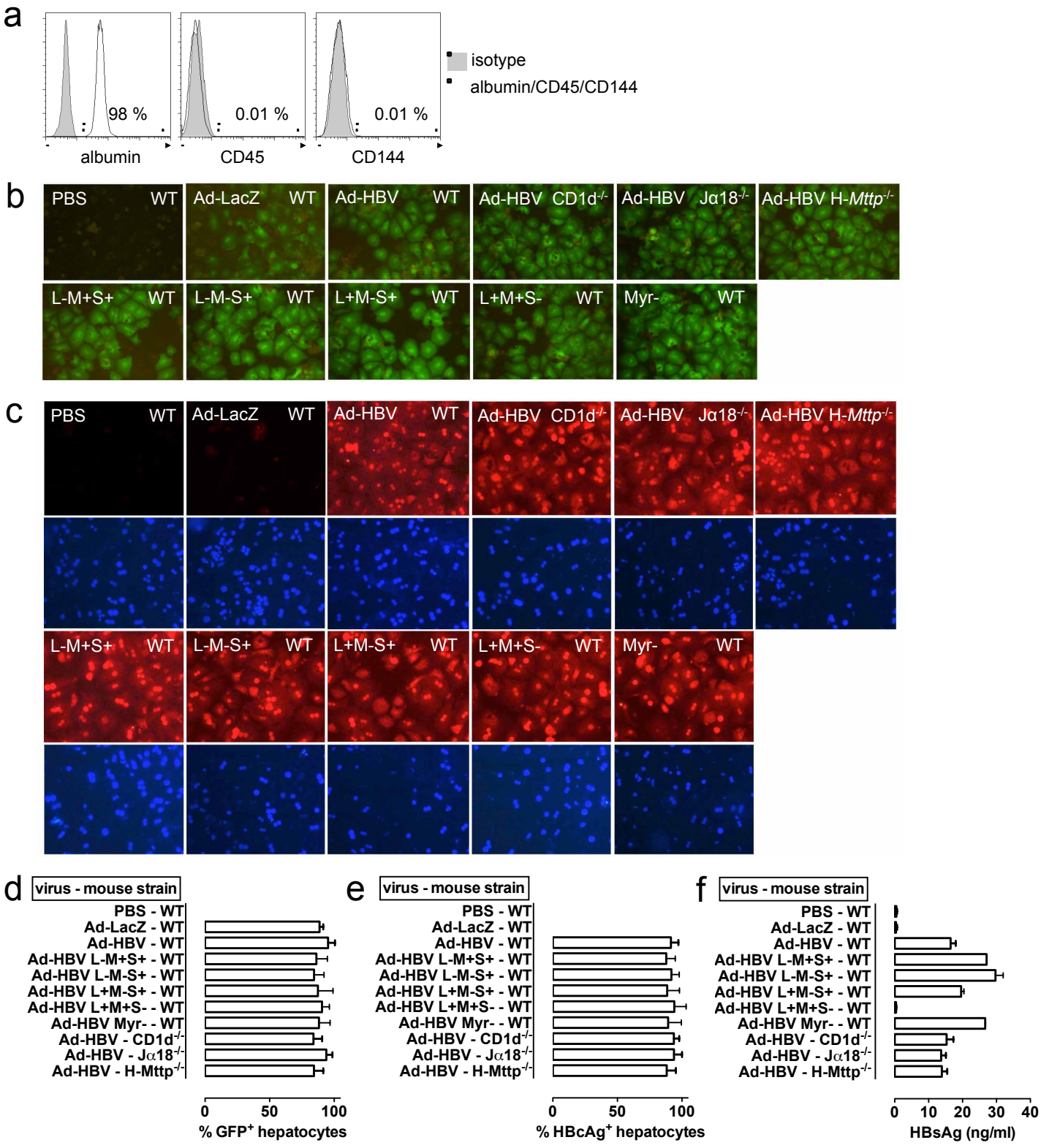

Suppl. Fig. 9. (a) Histograms of primary C57BL/6J hepatocytes stained for the hepatocyte marker albumin (intracellular), the leukocyte marker CD45, and the endothelial marker CD144. Gates indicate the percentage of positive cells. Similar observations were made with CD1d$^{-/-}$, Jα18$^{-/-}$, and H-*Mttp*$^{-/-}$ hepatocytes. (b-f) Immunofluorescence of GFP (b), HBcAg (c, upper panel), and DAPI (c, lower panel) in primary hepatocytes of the indicated mouse strains (upper right corner) 48h after transduction with the indicated viruses (upper left corner). (d-e) Percentage (mean ± s.e.m.) of hepatocytes positive for GFP (d) and HBcAg (e). f) Concentration of HBsAg secreted by primary hepatocytes as determined by ELISA. Results are representative of two independent experiments.

Nature Medicine doi:10.1038/nm.2811

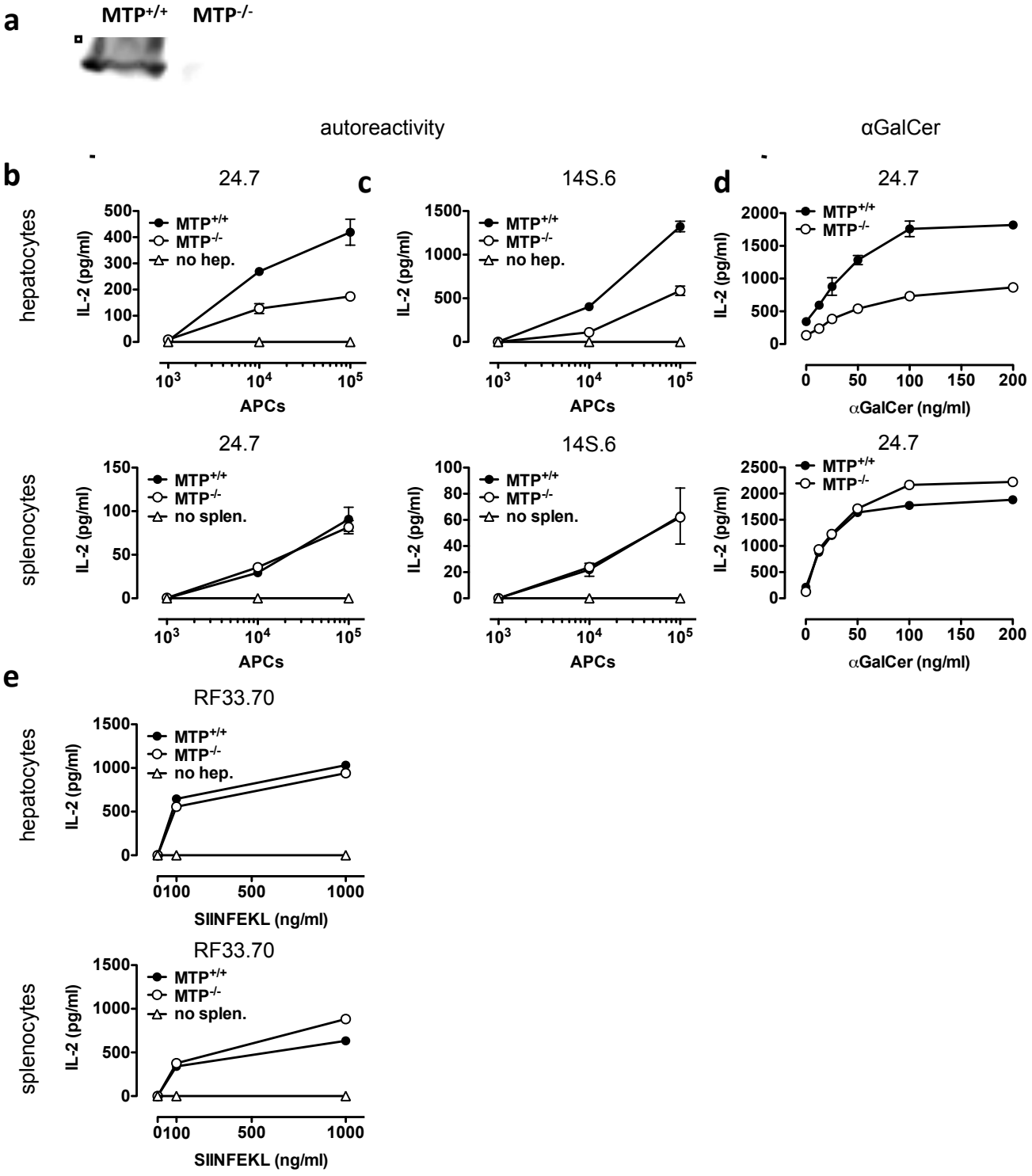

Suppl. Fig. 10. Characterization of H-*Mttp*$^{-/-}$ mice. a) Western blot demonstrating MTP expression in whole cell lysates of perfused livers from H-*Mttp*$^{-/-}$ mice (MTP$^{-/-}$) and their Alb*Cre*-negative littermates (MTP$^{+/+}$). b-e) Presentation of endogenous antigens (b, c), αGalCer (d), and SIINFEKL (e) by the indicated antigen presenting cells obtained from H-*Mttp*$^{-/-}$ mice (MTP$^{-/-}$) and Alb*Cre*-negative littermates (MTP$^{+/+}$). IL-2 secretion by the invariant NKT hybridoma 24.7 (b, d), the non-invariant NKT hybridoma 14S.6 (c) and the MHC-class I-restricted T cell hybridoma RF33.70 (e) was determined by ELISA after 24h of coculture. Mean ± s.e.m. of triplicate cultures are shown. Results are representative of three independent experiments.

Nature Medicine doi:10.1038/nm.2811

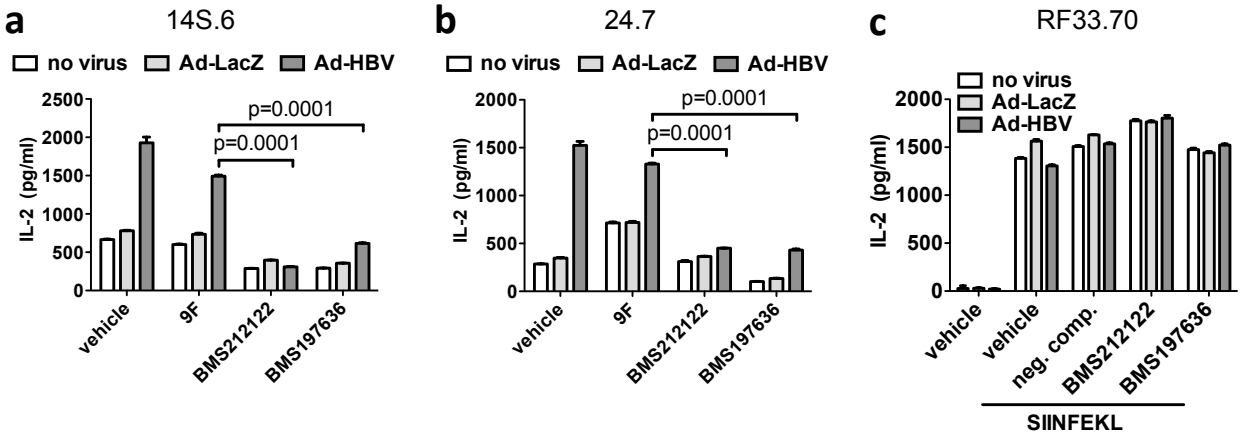

Suppl. Fig. 11. Ad-HBV-induced NKT activation by hepatocytes is dependent on MTP. Wildtype C57BL/6J hepatocytes were infected as indicated *in vitro*, treated with the indicated MTP-inhibitors or the structurally related control compound 9-fluorenyl carboxylic acid (neg. comp.) and were cocultured 72h after infection and 48h after beginning of MTP inhibitor treatment with the non-invariant NKT hybridoma 14S.6 (a), the invariant NKT hybridoma 24.7 (b) or the SIINFEKL-reactive T cell hybridoma RF33.70 (c). IL-2 secretion was determined by ELISA after 16h of coculture. Mean ± s.e.m. of triplicate cultures are shown. Results are representative of three independent experiments.

Nature Medicine doi:10.1038/nm.2811

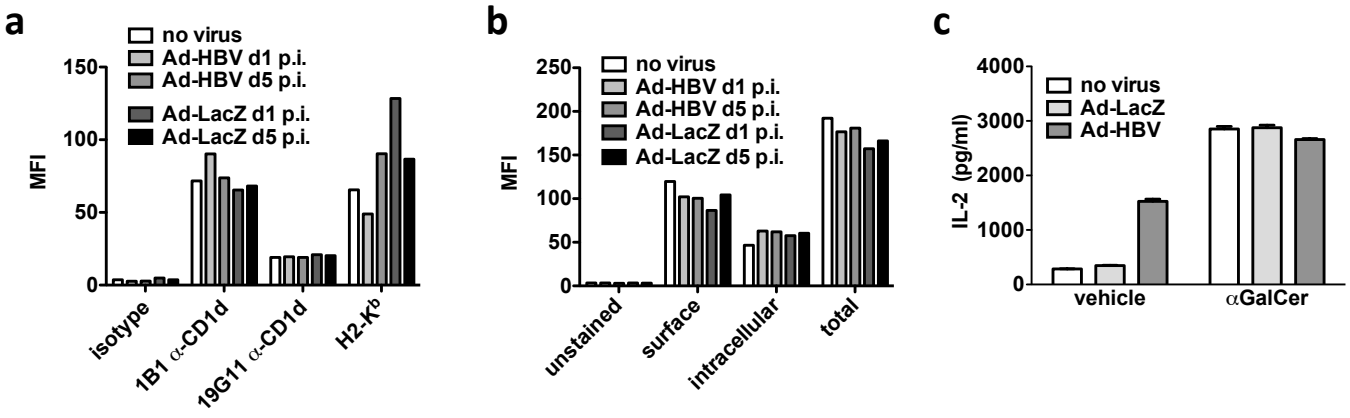

Suppl. Fig. 12. HBV-induced NKT activation is not due to altered CD1d expression of hepatocytes. (a-b) Unaltered cell surface (a) and intracellular (b) CD1d (a-b) and MHC class I (H2-K^b, a) expression by hepatocytes as determined by flow cytometric analysis of primary hepatocytes from mice infected *in vivo* with Ad-HBV and Ad-LacZ. Shown is the mean fluorescence intensity. 1B1 and 19G11 are different antibody clones directed against murine CD1d. Analyses in (b) are based on 1B1 staining. (c) Unaltered presentation of αGalCer (100 ng/ml) by hepatocytes to the 24.7 iNKT hybridoma. Hepatocytes were obtained two days after infection with Ad-HBV and Ad-LacZ *in vivo*. IL-2 release was determined by ELISA after 16h of coculture. Mean ± s.e.m. of triplicate cultures are shown. Results are representative of three independent experiments.

Nature Medicine doi:10.1038/nm.2811

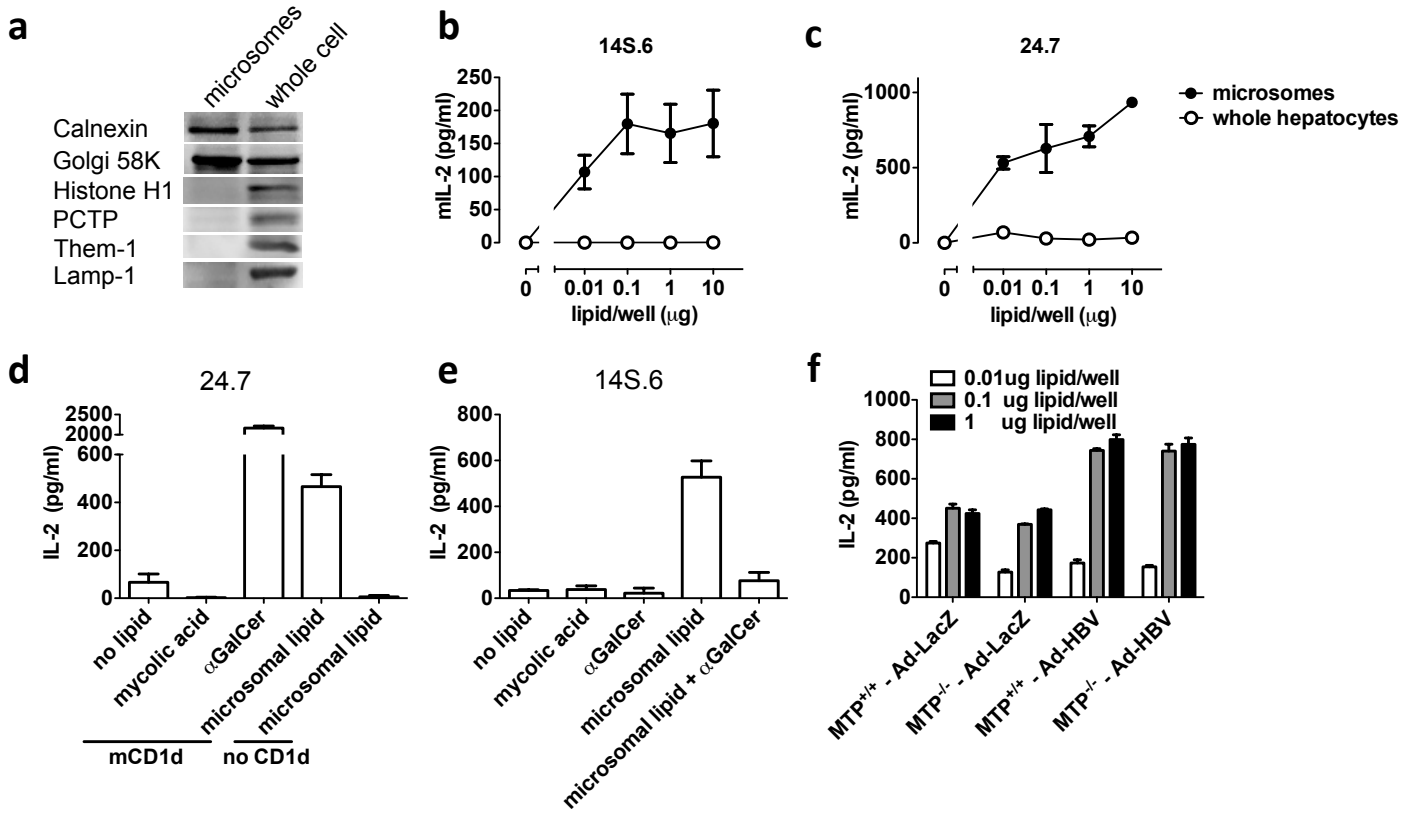

Suppl. Fig. 13. Activation of NKT cells by microsomal lipids of Ad-HBV but not Ad-LacZ infected hepatocytes. (a) Western blots of microsomal preparations and whole cell lysates demonstrating endoplasmic-reticulum origin of microsomal preparations. (b-c) Lipids extracted from hepatocyte microsomes or whole hepatocytes were loaded onto plate-bound CD1d. After removal of unbound lipids, non-invariant 14S.6 (b) and invariant 24.7 (c) NKT hybridomas were added. (d-e) Presentation of microsomal lipids by plate-bound CD1d as described in (b-c). In addition, lack of NKT activation by the CD1b-binding lipid mycolic acid is shown as well as lack of NKT activation by microsomal lipids in the absence of CD1d. Furthermore, incubation with an excess of the selective iNKT antigen αGalCer after loading of microsomal lipids completely inhibited activation of non-αGalCer-reactive 14S.6 demonstrating competition for CD1d binding. (f) Presentation of microsomal lipids obtained from primary hepatocytes of the indicated strains obtained two days after *in vitro* infection with the indicated viruses. CD1d presentation to non-invariant 14S.6 is shown. IL-2 release by hybridomas was determined after 16h of coculture by ELISA. Mean ± s.e.m. of triplicate cultures are shown. Results are representative of three independent experiments.

Nature Medicine doi:10.1038/nm.2811

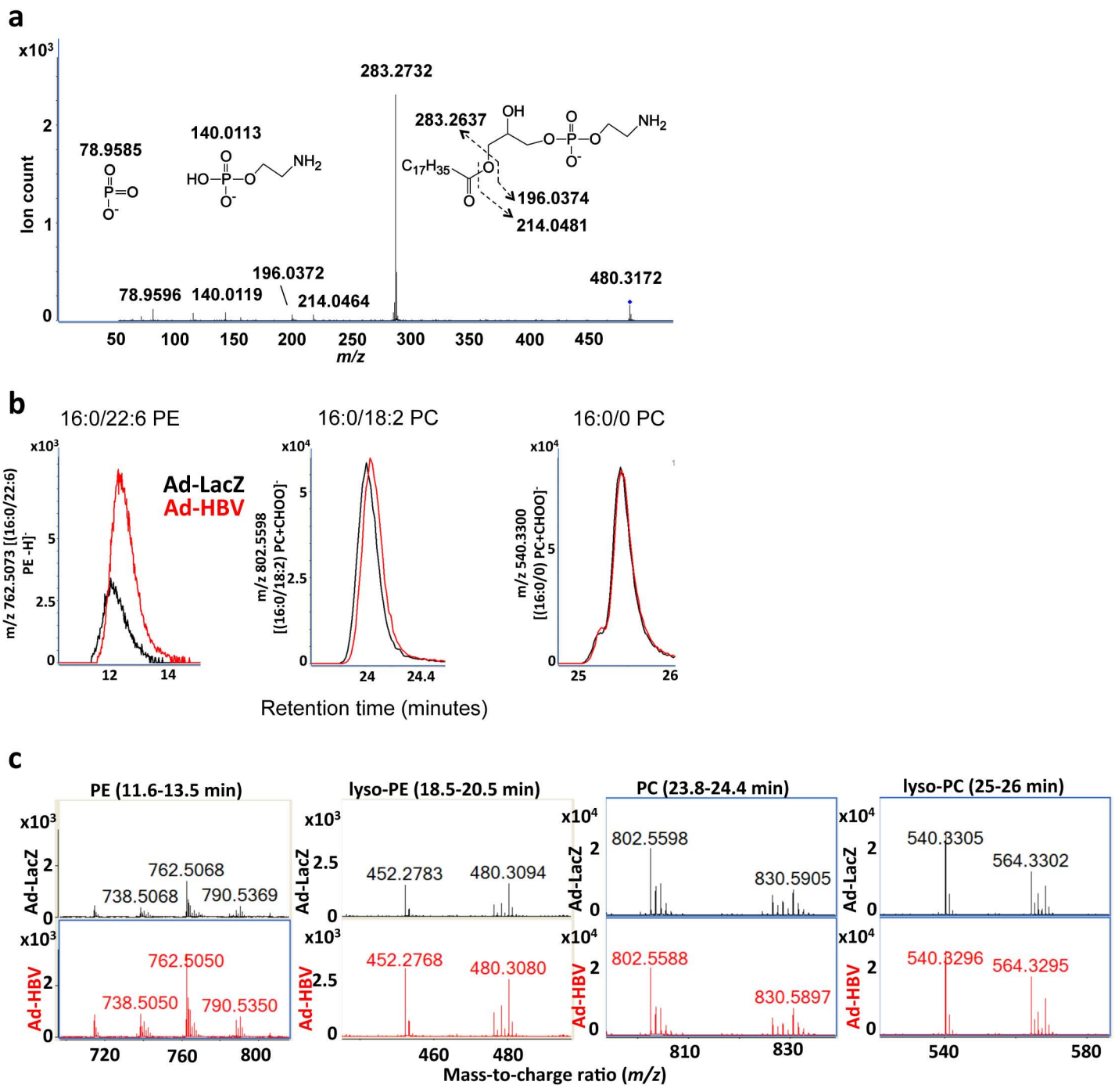

Suppl. Fig. 14. Phosphatidylethanolamine and phosphatidylcholine species in microsomes of Ad-HBV and Ad-LacZ-infected hepatocytes. (a) Collision induced dissociation of 480.317 in the negative mode yields ions expected for the phosphatidylethanolamine, glycerophosphoethanolamine, a C18 fatty acyl unit and other indicated produces of lysoPE. (b) Extracted ion chromatograms corresponding to the mass of the most abundant species of posphatidylethanolamine, phosphatidylcholine and lyso-phosphatidylcholine after injection of normalized total lipids from Ad-HBV and Ad-LacZ microsomes. (c) Mass spectra derived from the indicated elution times that correspond to peak abundance of the indicated lipid show ions that illustrate mass intervals expected for an alkane series, unsaturation and isotopes.

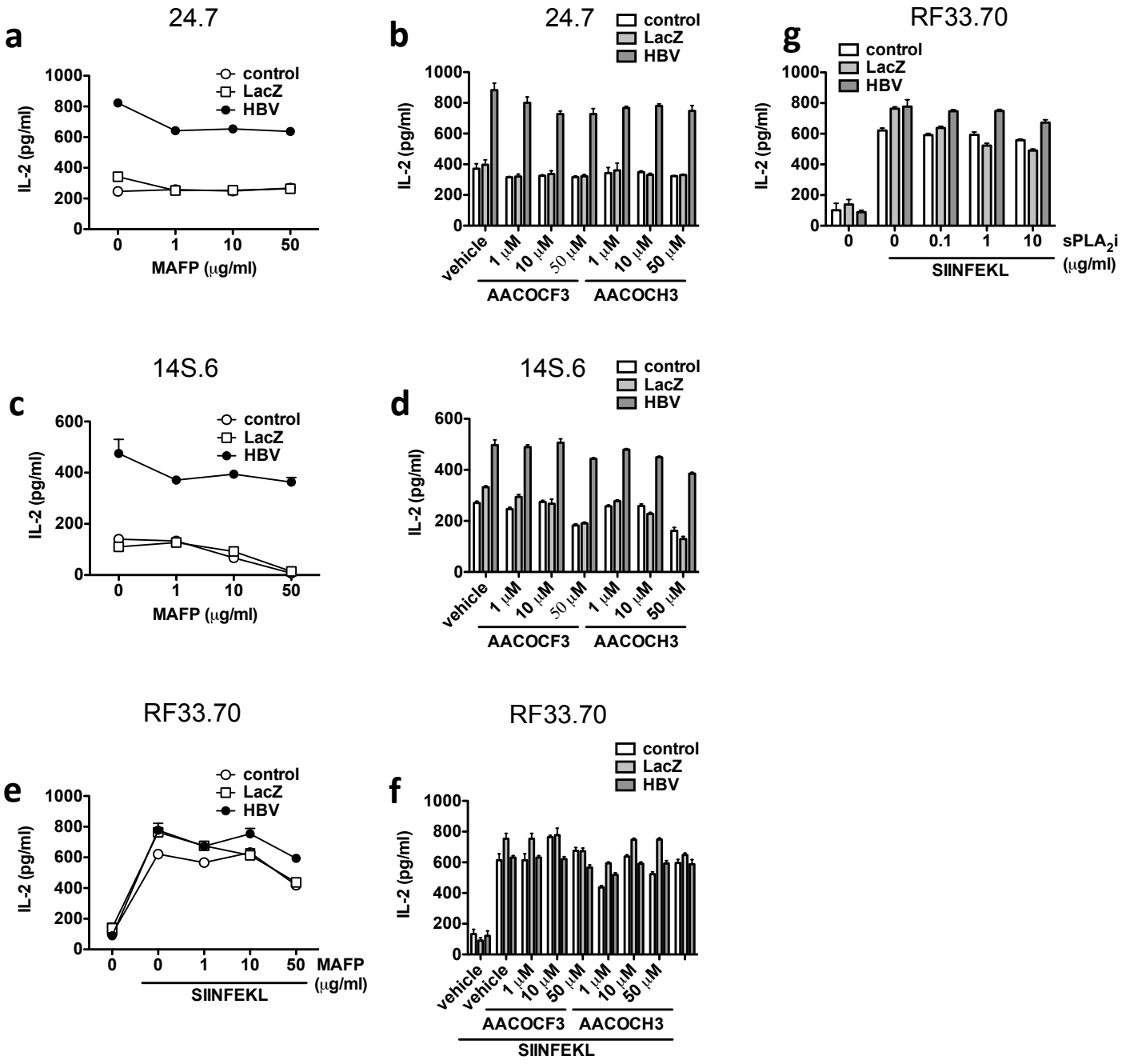

Suppl. Fig. 15. Unaltered HBV-induced NKT cell activation upon inhibition of $cPLA_2$ enzymes and unaltered MHC class I presentation upon $sPLA_2$ inhibition. Primary hepatocytes from wildtype C57BL/6J mice were infected with Ad-HBV or Ad-LacZ and were treated with the indicated $cPLA_2$ inhibitors (a-f, MAFP, AACOCF3), negative control (AACOCH3, b, d, f), and $sPLA_2$ inhibitor (g) for 12 h before addition of the invariant NKT hybridoma 24.7 (a, b), the non-invariant NKT hybridoma 14S.6 (c, d) or the MHC class I-restricted hybridoma RF33.70 (e, f, g). IL-2 release by hybridomas was determined 16 h after their addition to plates. Mean ± s.e.m. of triplicate cultures are shown. Results are representative of three independent experiments.

Nature Medicine doi:10.1038/nm.2811

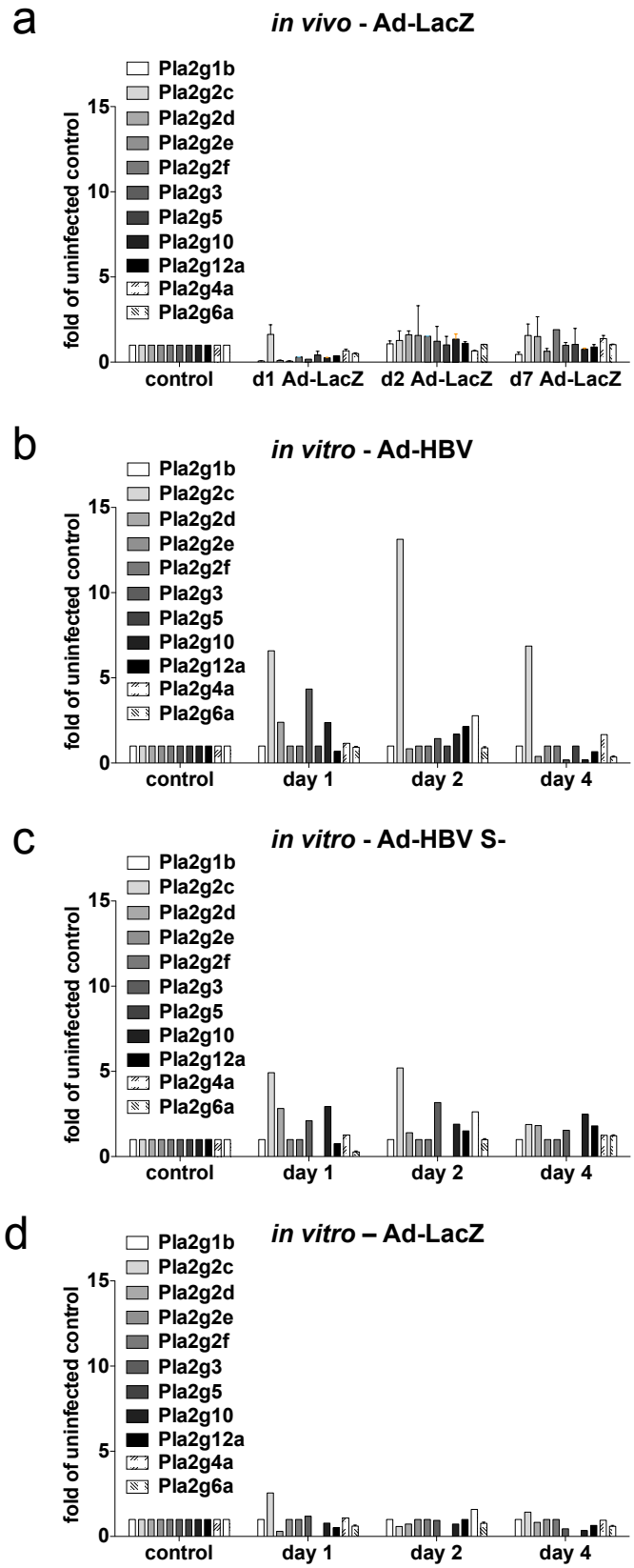

Suppl. Fig. 16. Regulation of PLA_2 expression *in vivo* (a) and *in vitro* (b-d). a) Expression of PLA_2 transcripts in murine livers following *in vivo* infection with Ad-LacZ. Livers were perfused prior to RNA extraction to remove blood cells. (b-d) HBV-induced regulation of phospholipases in primary hepatocytes *in vitro*. Primary hepatocytes from wildtype C57BL/6J mice were infected with Ad-HBV (b), Ad-HBV expressing mutant small HBsAg (Ad-HBV S-, c), and Ad-LacZ (d), RNA was extracted at the indicated time points, and PLA_2 expression was determined by qPCR. Results are representative of two independent experiments.

Nature Medicine doi:10.1038/nm.2811

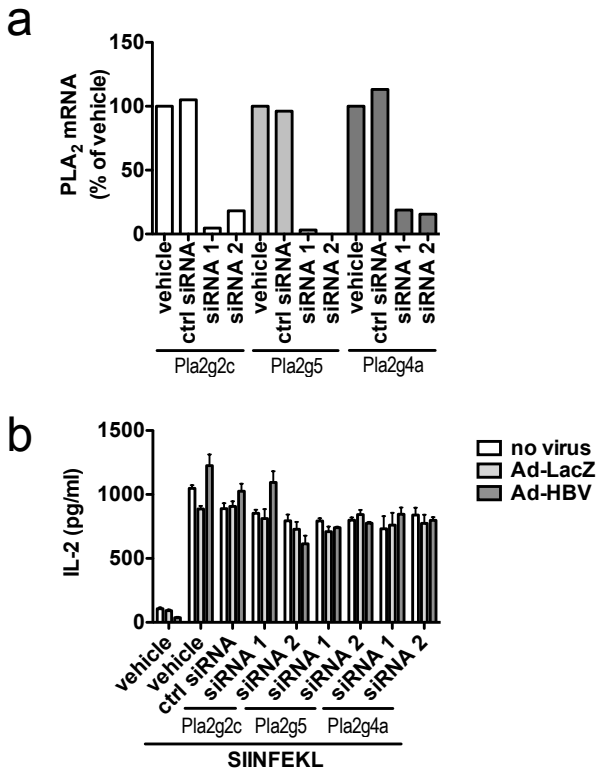

Suppl. Fig. 17. siRNA-mediated regulation of $sPLA_2$. (a) Primary hepatocytes obtained from wildtype C57BL/6J mice were transfected with siRNA directed against the indicated targets and PLA_2 expression was determined after 48h by qPCR. The two most potent siRNAs directed against each target are shown and were used for subsequent experiments as shown in Fig. 5i-j. The respective siRNAs were specific for each target and did not affect expression of other $sPLA_2$ enzymes as determined by qPCR (data not shown). (b) siRNAs directed against PLA_2 enzymes do not affect MHC class I-restricted antigen presentation. Primary hepatocytes were infected with Ad-LacZ and Ad-HBV and were transfected with siRNA as described above before loading with SIINFEKL and coculture with MHC class I-restricted T cells. Mean ± s.e.m. of triplicate cultures are shown. Results are representative of two independent experiments.

Nature Medicine doi:10.1038/nm.2811

a

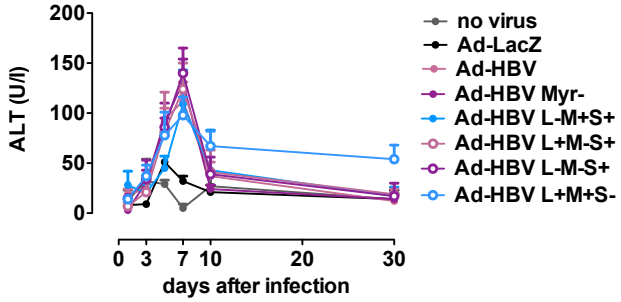

b

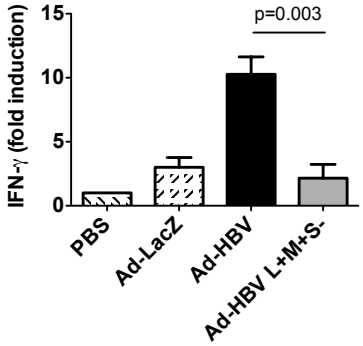

c

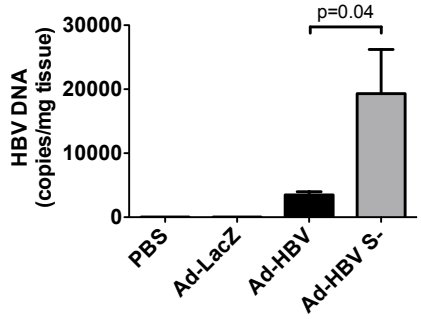

Suppl. Fig. 18. Small HBsAg deficiency is associated with chronicity of infection. (a) Mice were injected with HBV mutants and ALT(a), liver IFN-γ mRNA levels (b, d5), and liver HBV DNA (c, d10) were determined as described in Figure 2. Mean ± s.e.m. is shown (4-6 mice/group). Results are representative of two independent experiments.

Nature Medicine doi:10.1038/nm.2811

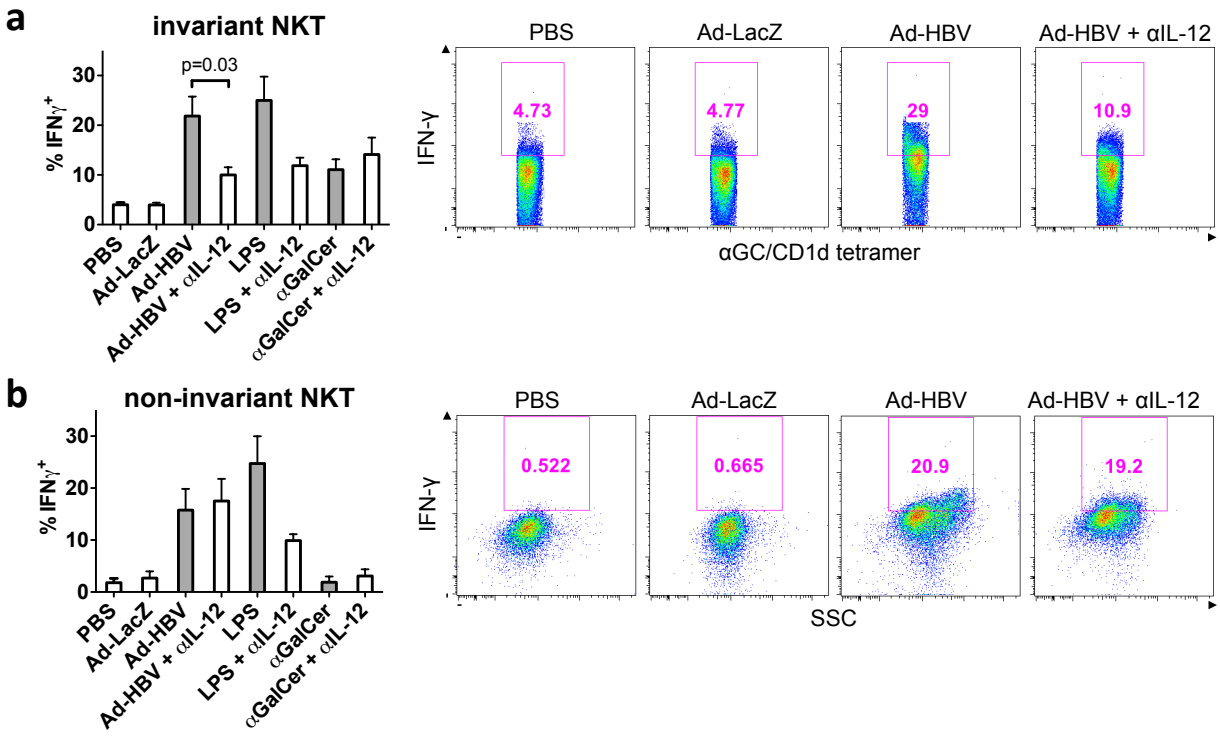

Suppl. Fig. 19. Direct and indirect mechanisms of NKT cell activation in response to Ad-HBV *in vivo*. 4Get mice were injected with the indicated viruses, LPS and αGalCer in the presence or absence of antibody-mediated IL-12 neutralization. Liver mononuclear cells were obtained 6 hours (αGalCer) and 24 hours (viruses, LPS) after stimulation and the percentage of IFN-γ-producing cells was determined by flow cytometric analysis of GFP$^+$ αGalCer/CD1d-tetramer$^+$ CD3$^+$ invariant NKT cells (a) and GFP$^+$ αGalCer/CD1d-tetramer$^-$ CD3$^+$ non-invariant NKT cells (b). Lack of CD69 upregulation of non-invariant NKT cells in response to αGalCer confirms that these cells are non-invariant NKT cells and not iNKT cells that escaped tetramer recognition due to activation-induced TCR downregulation. Representative histograms and dot plots are shown. Bar graphs show mean ± s.e.m.. Results are representative of two independent experiments.

Nature Medicine doi:10.1038/nm.2811

PRIMER NAME	SEQUENCE (5'-3')
mIFNg_F	ATGAACGCTACACACTGCATC
mIFNg_R	TCTAGGCTTTCAATGACTGTGC
mPLA2a2_F	CTGTTCTGCAAACCAGAACTC
mPLA2a2_R	GGGTAGAACTGGTACTTTAAACTG
mPLA2g1b_F	GTGTGGCAGTTCCGCAATATG
mPLA2g1b_R	CCTGTCTAAGTCGTCCACTGG
mPLA2g2c_F	GCTGCCAACCCATCTTGAATG
mPLA2g2c_R	CACAGACTGTTTGTCACACTCA
mPLA2g2d_F	TGCTGGCCGGTATAACTGC
mPLA2g2d_R	CTGTGGCATCTTTGGGTTGC
mPLA2g2e_F	CCAGTGGACGAGACGGATTG
mPLA2g2e_R	AGCAGCTCTCTTGTCACACTC
mPLA2g2f_F	ACTGGACGGAAGAGCCCAA
mPLA2g2f_R	GGATGGAGTTTCTGTGTGTGAT
mPLA2g3_F	AGAGACCACAGGGCCATTAAG
mPLA2g3_R	GCTGTAGAATGACATGGTGCT
mPLA2g4a_F	CAGCACATTATAGTGGAACACCA
mPLA2g4a_R	AGTGTCCAGCATATCGCCAAA
mPLA2g5_F	CCAGGGGGCTTGCTAGAAC
mPLA2g5_R	AGCACCAATCAGTGCCATCC
mPLA2g6a_F	GCAAGCTGATTACCAGGAAGG
mPLA2g6a_R	GAGAGAAGAGGGGGTGAGTTG
mPLA2g10_F	GTGCAGGTGTGACGAGGAG
mPLA2g10_R	CACTTGGGAGAGTCCTTCTCA
mPLA2g12a_F	AGATAGACACGTACCTCAACGC
mPLA2g12a_F	GCTGCACTTGTACTGGCAGA
mBACTIN_F	GATGCTCCCCGGGCTGTATT
mBACTIN_R	GGGGTACTTCAGGGTCAGGA
hPLA2G1B_F	TGTGGCAGTTCCGCAAAATG
hPLA2G1B_R	GCCGTAGTTGTTGTATTCCAAGA
hPLA2G2A_F	GAAAGGAAGCCGCACTCAGTT
hPLA2G2A_R	CAGACGTTTGTAGCAACAGTCA
hPLA2G2D_F	TCCACTGCTCTGACAAGGGAA
hPLA2G2D_R	CAGTCGCTTCTGGTAGGTGT
hPLA2G2E_F	TCAGCGAACGTGGCATTTTCT
hPLA2G2E_R	TGGGCATATTTGCGGTTGTAG
hPLA2G2F_F	ACCAGACGTACCGAGAGGAG
hPLA2G2F_R	CGCTGGGGATTGGTGACTG
hPLA2G3_F	CACCCTTGCAGTACAACTATGG
hPLA2G3_R	TGGAGTCGTGCTGATTCTGTAG
hPLA2G4a_F	GATGAAACTCTAGGGACAGCAAC
hPLA2G4a_R	CTGGGCATGAGCAAACTTCAA
hPLA2G6a_F	GTGGACACCCCGAATGACTTT
hPLA2G6a_R	CCTGTAGTTGTCTGCCGATTT
hPLA2G10_F	AACCCCCATCGCCTATATGAA
hPLA2G10_R	TCGAGTGTAACAACAGTCGTG
hBACTIN_F	GATGAGATTGGCATGGCTTT
hBACTIN_R	CACCTTCACCGTTCCAGTTT
HBV469U	CCCGTTTGTCCTCTAATTCC
HBV569L	GTCCGAAGGTTTGGTACAGC

Suppl. Table 1. Primer sequences

Nature Medicine doi:10.1038/nm.2811